DISPERSION DEFORMATION OF OPTOACOUSTIC PULSES IN THE SURFACE LAYER OF THE OCEAN

V. D. Kiselev and A. O. Maksimov

UDC 534.222.2

1. Introduction. The application of lasers to generate acoustic pulses under natural conditions [1-3] has made it possible to reveal a number of differences in the shape of the received acoustic signals in comparison with the signals recorded under laboratory conditions for fresh water [4-6]. The principal distinction between conditions of natural and laboratory experiments is the presence of a concentration of gas bubbles in the surface layer of the ocean. Resonance scattering by bubbles leads to substantial dispersion of acoustic waves. In the present study we provide a theoretical description of dispersion deformation of optoacoustic pulses due to the presence of gas bubbles. It must also be noted that the occurrence of dispersion effects is rendered favorable by the fact that laser sources make it possible to obtain pulses of very short duration. Components with substantially different evolution laws appear in the very wide spectrum of this signal, which, in turn, leads to the appearance of distortions.

In constructing the theory of this effect we consider a situation similar to the experimental conditions [1, 3], when the source is a CO_2-laser beam of radius $a \sim 10^{-2}$ m, wave length $\lambda_0 = 10^{-5}$ m, and pulse duration $\tau_L \sim 10^{-5}$ sec. Keeping in mind the oceanographic applications, particularly the realization of the distant sounding method, we analyze in detail the generation mechanism, implemented with explosive boiling and guaranteeing substantially more effective transformation of electromagnetic into acoustic energy than by thermoelastic or evaporating mechanisms. It must be noted that the theory of excitation of optoacoustic signals in a homogeneous two-phase medium was developed earlier [7] for the thermoelastic generation mechanism.

Taking into account the gas bubbles distributed in the liquid leads to substantial dispersion of acoustic waves:

$$k^2 = \frac{\omega^2}{c_\infty^2}\,[1 + \chi(\omega)], \quad \chi(\omega) = 4\pi c_\infty \int_0^\infty \frac{g(R_0, z)\, R_0 dR_0}{\omega_0^2(R_0) - \omega^2 + 2i\delta_0\omega}. \tag{1.1}$$

Here k is the wave number, ω is the frequency, c_∞ is the speed of sound in a pure liquid, $\chi(\omega)$ is the susceptibility ($|\chi(\omega)| << 1$), $g(R_0, z)$ is the bubble distribution function in size, R_0 is the bubble radius, $\omega_0(R_0)$ is the eigenfrequency, and δ_0 is the attenuation constant. The bubble distribution in the surface layer is extremely inhomogeneous over depth. According to contemporary concepts [8-10], $g(R_0, z) = g(R_0)\exp(-|z|/d)$ ($d \sim 2$ m), and therefore the results of [7] cannot be applied directly.

At the same time the geometric sizes of optoacoustic pulses under the conditions considered consist of several centimeters, making it possible to use the "geometric acoustics" approximation to describe their evolution. In this case one obtains the following expression for the radiation field at the illuminated spot

$$P(z, t) = -i\frac{a^2}{2c_\infty z}\int \frac{d\omega}{2\pi}\,\omega\tilde{\mathcal{F}}(\omega)\exp\left\{i\omega\left[\frac{d_*\chi(\omega, 0)}{2c_\infty} - \left(t - \frac{z}{c_\infty}\right)\right]\right\}, \tag{1.2}$$

where $d_* = d(1 - \exp(-|z|/d))$. For the surface layer $P_s(\rho, t)$, modeling the recoil of fluid vapor boiling under the action of laser radiation, we adopt the traditional assumption of factorization of spatial and temporal dependences: $P_s(\rho, t) = \bar{P}_s(\rho)\cdot \mathcal{F}(t)$, where $a^2 = \pi^{-1}\int d\rho \bar{P}_s(\rho)$, $\tilde{\mathcal{F}}(\omega)$ is the Fourier component of the temporal envelope.

2. The Model. The shape of the susceptibility $\chi(\omega, z)$ depends the bubble size distribution (1.1). Figure 1 shows a number of bubble size distributions, obtained on the basis of both acoustic [9, 11] (curves 1, 2) and optical [12-14] (curves 3-5)

Vladivostok. Translated from Prikladnaya Mekhanika i Tekhnicheskaya Fizika, No. 6, pp. 57-64, November-December, 1993. Original article submitted March 12, 1992; revision submitted November 11, 1992.

0021-8944/93/3406-0796$12.50

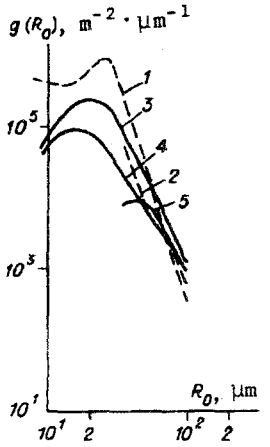

Fig. 1

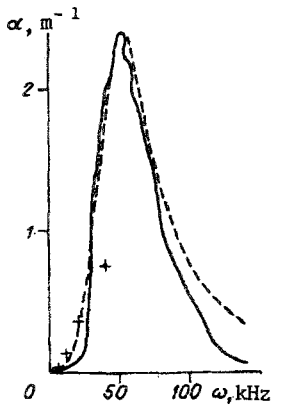

Fig. 2

measurements of comparable recording conditions of wind velocity W (of surface agitation) and depth. Attempts of approximating these distributions by simple analytic expressions, in which the dependence on external conditions is reflected only by characteristic scales and special points, were undertaken in [8, 15, 16]. It must be noted, however, that these models are based exclusively on the data of [12]. An obvious confirmation of the self-consistency of distributions is the calculation on their basis of the dispersions in sound velocity and attenuation, which are directly measurable in acoustic experiments. Figure 2 illustrates these calculations on the example of the frequency dependence of the attenuation coefficient. The solid curve is the calculation [15]. The values were recalculated for the ocean surface and for a wind velocity W = 12 m/sec.

Based on the results of [8, 15 16], it is suggested to use a relatively simple analytic expression, in which the dependence on external conditions is depicted by a small number of parameters for approximating not the distribution function itself, but the susceptibility $\chi(\omega, 0)$:

$$\chi(\omega, 0) = \frac{F\omega_*^2}{\omega_*^2 - \omega^2 - 2i\delta_*\omega}. \tag{2.1}$$

The choice of the given approximate expression is determined by the fact that it has the same functional dependence for the low- and high-frequency asymptotes as the exact integral representation (1.1). Besides, Eq. (2.1) leads to the same characteristic type of bell-shaped curve as a function of $\alpha = \mathrm{Im}\, k = (\omega/2c_\infty)\, \mathrm{Im}\, \chi(\omega, 0)$ as Eq. (1.1). The values of the adjustable parameters ω_*, δ_*, and F were found from the following conditions: ω_* corresponds to max $\alpha(\omega)$, while F and δ_* are determined from the relations

$$F = -2\Delta c(0)/c_\infty, \quad F\omega_*^2/(4\delta_* c_\infty) = \alpha(\omega_*)$$

$$(\Delta c(0) = -(c_\infty/2)\, \mathrm{Re}\, \chi(0, 0), \quad F = 4\pi c_\infty \int_0^\infty dR_0 R_0 g(R_0)\, \omega_0^{-2}(R_0)).$$

To estimate these quantities we used the data of [8, 9, 15, 16]. Based on the model of bubble size distribution, the function $\alpha = \alpha(\omega)$ was calculated in [15], in which case the value of max α, reduced to the surface of the ocean, was $\alpha(\omega_*, 0) = 2.4\ \mathrm{m}^{-1}$. Unfortunately, that study does not contain a correction to the speed of sound. A similar calculation is contained in [16] for the frequency interval 0 to 40 kHz (these data are denoted by + in Fig. 2), but the value $\Delta c(0) = -27$ m/sec, corresponding to a wind velocity W = 11-13 m/sec, creates doubts about too high a value of this quantity. The reason for the doubt is the comparison with the data of [17], where for the bubble concentration, substantially exceeding the conditions of [12], the $\Delta c(0)$ value did not exceed 19 m/sec (at the frequency 5 kHz). Recalculation at comparable concentrations leads to $\Delta c(0) = -17$ m/sec. Direct calculations of F for the model bubble distribution of [8] also provide the same order of magnitude. Using these estimates, we obtained the following adjustable parameter values: $\omega_*/2\pi = 50$ kHz, $\delta_* \approx 0.5\omega_*$, $F = 2.3 \cdot 10^{-2}$. Figure 2 illustrates the behavior of the function $\alpha = \alpha(\omega)$ in the model (2.1) by the dashed line. It is noted that, judging from recent data (see Fig. 1), the methodology of [12] reduces the bubble concentration in the small size region, so that the maximum of the distribution $g(R_0)$ settles down more quickly in the region $R_0 = 2 \cdot 10^{-5}$ m, which, in turn, must lead to a shift in max $\alpha(\omega)$ toward the high-frequency region. Nonetheless, due to the absence of both analytic models, and calculations on their basis of damping and corrections to the speed of sound, in what follows we are concerned with the estimates given above.

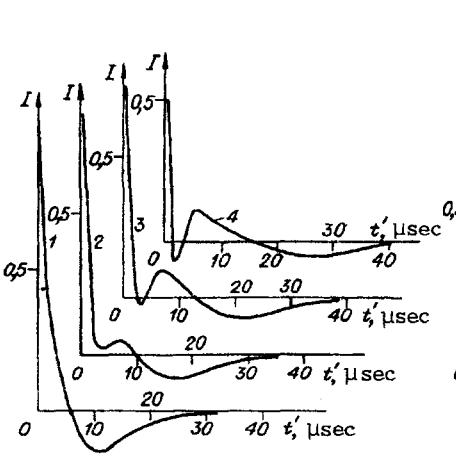

Fig. 3

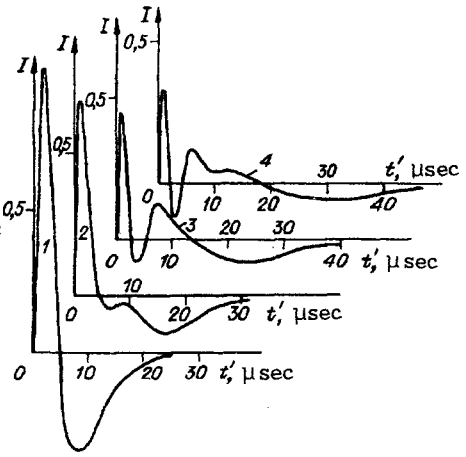

Fig. 4

The next step consists of specifying the temporal envelope of the source. Unlike the thermoelastic mechanism, in the regime of explosive boiling there is no longer a unique correspondence between the shape of the laser pulse and the temporal envelope of the source. In this case the set of models [5, 6, 18-22], used for the characteristics of a CO_2-laser pulse, cannot be applied directly. We intend to discuss three characteristic features in the shape of the envelope and, consequently, the radiated acoustic pulse: the generation law, the characteristic duration, and the decay law.

The Gaussian model $\mathcal{F}(1) = P_0 \exp(-t^2/\tau_L^2)$ is unsuitable for our purposes. The infinite extent of the front does not make it possible to manifest the spatial distinction of the spectral components propagating with different velocities, which is essentially also one of the effects to be discussed – a distinct signature [23].

The formal representation of a pulse of finite extent in the form of a Fourier series and the structure analysis of separate component contributions are the traditional path [24], and lead to a completely determined front structure: in the absence of dispersion the leading and rear fronts of the separate harmonics have the form of a step. Any other generation law necessarily requires a complicated scheme and the inclusion of several harmonics.

It is particularly important to dwell on the description of the lead front since, as follows from [3], complicated physical effects, related to possible secondary generation of an acoustic pulse in the region of explosive boiling, can influence the pattern of transient processes. So as not to get involved with this deficiency in the present study, we assume an exponential decay law.

Thus, to describe the time dependence of the source it is suggested to use one of three models ($\mathcal{F}(t) = P_0 \exp(-t/\tau_L)$ (t/τ_L) [5], $\mathcal{F}(t) = 2.5P_0(t/\tau_L)^2 \exp(-t^2/\tau_L^2)$ [6], $\mathcal{F}(t) = P_0(3t/\tau_L)^3 \exp(-3t/\tau_L)$ [21, 22]), having different generation laws (step, linear, and quadratic) and characterized by a single parameter – the duration. In this case the Fourier transform $\tilde{\mathcal{F}}(\omega)$ appearing in the integral (1.2) is described by the expression $\tilde{\mathcal{F}}(\omega) = in!\,(in/\tau_L)^n/(\omega + in/\tau_L)^{n+1}$, n = 1, 2, 3, where the model of [6], having a complicated analytic behavior, is replaced by the simpler approximation $\mathcal{F}(t) = P_0(2t/\tau_L)^2 \exp(-2t/\tau_L)$, leading to the same linear generation law, but at the same time possessing a simple analytic structure for n = 2.

3. The Signature. We turn now directly to determining the evolution of the optoacoustic pulse. In this case it is convenient to measure time from the moment of pulse generation $t' = t - |z|/c_\infty$ and transform to the dimensionless variables $\xi = \omega/\omega_*$, $\tau = t'(2c_\infty/Fd_*)$, $\nu = \delta_*/\omega_*$. It is also meaningful to distinguish a parameter characterizing the dispersion deformation, $\lambda = Fd_*\omega_*/2c_\infty$. In this case the expression for the pressure in the far-field zone on the optical radiation axis (1.2) acquires the form

$$P(z, \tau) = \frac{a^2 P_0}{2zc_\infty \tau_L} I, \quad I = \frac{i^n nn! m_n^{n-1}}{2\pi} \int_{-\infty}^{+\infty} d\xi \exp(\lambda\Phi(\xi, \tau)) \frac{\xi}{(\xi + im_n)^{n+1}}, \tag{3.1}$$

$$\Phi(\xi, \tau) = i\xi\,[(1 - \xi^2 - 2i\nu\xi)^{-1} - \tau].$$

Starting with the fundamental studies of Sommerfeld and Brillouin, expressions of similar type were used to analyze the distortion of wave packets traversing through resonance media. An approximate analytic calculation of the integral (3.1) is possible at short times ($\tau << 1$) and for substantial dispersion ($\lambda >> 1$), when the steepest descent method can be used [23, 24]. Since both approximations use deformation contour integration, it is necessary to present the structure and location of the critical points of the integrand expression.

Due to the causality principle all singular points of the integrand expression are located in the lower half-plane ξ. They include the pole of $\tilde{\mathcal{F}}(\xi)$ at the point $\xi = -im_n = -in/(\omega_*\tau_L)$ (depending on the model, this pole can be of order 2, 3, or

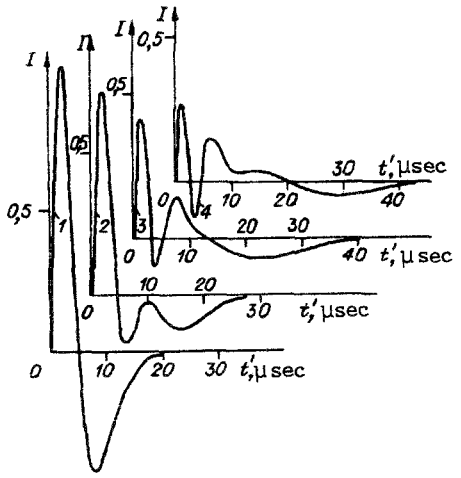

Fig. 5

4) and the two susceptibility poles $\xi_N = -i\nu \pm \sqrt{1-\nu^2}$. Here it must be noted that the expression $k = (\omega/c_\infty)(1 + \chi(\omega))^{1/2}$, appears in the original integral, therefore the use of the approximation $(1+\chi)^{1/2} \simeq 1 + \chi/2$ is possible not too closely to the poles and to the branching points of this expression. By the same reason the ξ plane contains, along with the singularities mentioned, branching points $(1 + \chi(\omega, 0) = 0)$, combining the branching points with the poles of $\chi(\omega, 0)$ [24].

Within the short time approximation ($\tau << 1$) one can describe the evolution of the leading front of the pulse, determined by the contribution of the high-frequency components, propagating with the highest velocities. For this purpose we deform the integration contour in the vicinity of the large radius $\xi \sim 1/\sqrt{\tau}$, $|\xi| << 1$, $\xi << m_n$, and the integral (3.1) acquires the form

$$P(z, \tau) = \frac{a^2 P_0 \omega_*}{2zc_\infty} n!\,(im_n)^n \oint \frac{d\xi}{2\pi} \frac{\exp\left[-i\lambda\left(\frac{1}{\xi} + \tau\xi\right)\right]}{\xi^n} = \tag{3.2}$$

$$= \frac{a^2 P_0 \omega_*}{2zc_\infty} n! m_n^n \tau^{(n-1)/2} J_{n-1}(2\lambda\sqrt{\tau}).$$

The appearance of an oscillating structure reflects the formation process of the signature, surpassing the basic portion of the pulse. It is noted that one can talk convincingly about a distinct signature only when one oscillation period of the Bessel function occurs at a time $t' << \tau_L$. The first zeros of J_0, J_1, and J_2 occur at $2\lambda\sqrt{\tau} = 2.4$, 3.8, 5.1. Using for these estimates the values d = 2 m, $F = 2.3\cdot10^{-2}$, $c_\infty = 1.5\cdot10^3$ m/sec, $\omega_*/2\pi = 50$ kHz, one obtains $t_0' = 0.9$; 2.3; 4.2 μsec.

To calculate (3.1) when $\lambda >> 1$ one can use the steepest descent method. In this case the problem reduces to determining the time-varying positions of saddle points and poles of the integrand expression (3.1). These quite unwieldy calculations clarify, however, the physical meaning of the changes in the pulse shape (the extraction of the high-frequency signature, propagating in a pure liquid with the speed of sound, as well as the formation of an energy-carrying pulse, moving with the group velocity), but will be omitted. The point is that under the experimental conditions [1, 3] the estimates of bubble concentration, and the estimates on their basis of the quantity λ, give $\lambda \sim 1$, rendering the asymptotic estimates unconvincing.

4. Results. The most complex model is the envelope model, corresponding to the value n = 1: the slow decay law of the integrand expression for $\xi \to \infty$ worsens the convergence substantially. In this connection one must take into account the following circumstance, affecting the evolution of the high-frequency components.

The decay of the bubble distribution function in the small size region ($R_0 << 2\cdot10^{-5}$ m) leads to a reduced susceptibility Im $\chi(\omega)$ and, starting with some frequency, it is necessary to take into account the dissipative processes of viscosity and thermal conductivity, which can be accounted for by further contributions to the dispersion law of acoustic waves [25]:

$$k = \frac{\omega}{c_\infty}\left[1 + F\omega_*^2/2\,(\omega^2 - \omega_*^2 - 2i\delta_*\omega) + ia'\omega^2\right],$$
$$a' = \frac{1}{2\rho' c_\infty^2}\left[(4/3\eta + \zeta) + \varkappa\,(1/C_V - 1/C_p)\right]. \tag{4.1}$$

The second term in expression (4.1) describes the bubble contribution ($\delta_* \approx 1/2\omega_*$), ρ' is the fluid density, η and ζ are the dynamic and bulk viscosity coefficients, $\varkappa$ is the heat conduction coefficient, C_V and C_p are the heat capacities, and for water

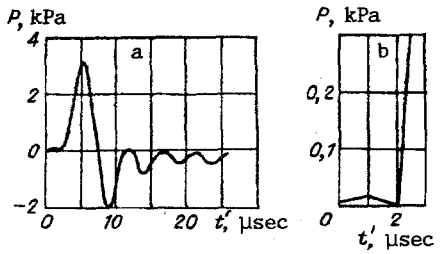

Fig. 6

$a_* = a'(2\pi)^2 = 0.024$ (μsec)^2/m. Therefore, these processes affect the damping of each Fourier harmonic over the whole ray propagation path, and an additional z-dependent factor appears in expression (3.2):

$$I = \frac{i^n n n! m_n^{n-1}}{2\pi} \int_{-\infty}^{+\infty} d\xi \frac{\xi \exp(\lambda\Phi(\xi, \tau))}{(\xi + im_n)^{n+1}} \exp(-a' z \omega_*^2 \xi^2).$$

Figure 3 shows calculation results, presenting signature formation with account of dissipative processes. The curves 2-4 correspond to the dissipative parameter values $\lambda = 1$, 2, and 3, while curve 1 describes the shape of the acoustic pulse in the absence of dispersion ($\lambda = 0$) and damping. The recording depth was taken equal to 8 m, and the constant characterizing pulse duration is $\tau_L = 5 \cdot 10^{-6}$ sec ($m_1 = 0.54$). The choice of the λ value was based on the tendency of obtaining a description within the same parameter region in which the asymptotic expansion method ceases to work ($\lambda >> 1$).

Now to describe the shape of the optoacoustic pulse for the models n = 2, 3 on the surface of force. In Figs. 4 and 5, the calculated results are presented for n = 2, $m_2 = 1.08$ and n = 3, $m_3 = 1.62$, respectively: $\tau_L = 5 \cdot 10^{-6}$ sec. Curve 1 corresponds with $\lambda = 0$ in neglecting dissipation, while curves 2-4 correspond to $\lambda = 1$, 3, and 5 if the dissipative process is taken into account. For convenience we compared a different model of the given dependence, normalized on the maximum pulse values at $\lambda = 0$.

Comparison of the calculation results in these three models shows that, as can be expected, the differences are primarily generated in the signature characteristics – its shape, amplitude, and duration. The flatter the leading front of the pulse (n = 1-3), the less are high-frequency components contained in its spectrum and correspondingly less is the amplitude of its signature. The signature formation process itself is also quite distinctive. Thus, in the model n = 1 substantial deformations occur during the compression of the acoustic pulse, and in the models n = 2, 3 – during the expansion phase.

To compare the calculation results with data of natural experiments we show in Fig. 6a the shape of observed [1, 3] optoacoustic pulses, and in Fig. 6b – fragments of the leading front structure. It is noted that it is precisely this portion of low amplitude compression, surpassing the basic portion of the pulse, and invariably present in the various series of measurements [1, 3], which initiated the appearance of theoretical studies. In the comparison one must select the most useful of the three envelope models of the surface force, as well as establish the characteristic values of the dispersion parameter λ and the duration of the surface force τ_L.

As follows from the calculations, the λ values must not exceed 3, since otherwise the dispersion spread of the pulse is too large. On the other hand, λ cannot be less than 1, since in the opposite case the signature cannot be formed.

The choice of the τ_L value is based on the fact that in the explosive boiling regime, and for optical pulse durations of 10^{-5} sec, the active time of effective surface force must be somewhat longer than this value, since following the cessation of action of laser radiation the heated spot continues exciting the sound field in the evaporation regime. Since τ_L determines the order of magnitude of the halfwidth of the surface force envelope, the calculations were carried out for $\tau_L = 5 \cdot 10^{-6}$ sec.

Finally, the selection of the surface force envelope is primarily determined by how any of these models reproduces the shape of the signature. Unfortunately, the low sensitivity of the adopted hydrophone GIR-1 in the high-frequency region reduces substantially the amplitude of the signature (Fig. 6b), thus rendering a unique selection quite difficult. The calculation with the model n = 3 leads to the smallest signature amplitude. To try to explain the divergence between the theoretical calculations and the measurement results, an attempt was undertaken in the present study of taking into account the deformations resulting from the hydrophone adopted by constructing model characteristics of the sensitivity on the basis of available amplitude-frequency characteristics. Unfortunately, the use of relatively simple models did not make it possible to formulate sufficiently adequate characteristics, therefore we do not provide the corresponding results.

It must be noted that the effect of singling out a signature in two-phase liquids was observed earlier [26, 27] for a monodisperse size distribution of bubbles in substantially different excitation regimes.

REFERENCES

1. O. A. Bukin, V. I. Il'ichev, and V. D. Kiselev, "Study of acoustic signals generated by a CO_2-laser in sea water," Dokl. Akad. Nauk SSSR, **315**, No. 1 (1990).
2. S. V. Egerev, L. M. Lyamshev, and K. A. Naugol'nykh, "Optoacoustic source in an oceanographic experiment," Akust. Zh., **36**, No. 5 (1990).
3. O. A. Bukin, V. I. Il'ichev, and V. D. Kiselev, "Observation of secondary generation of sound in a liquid with bulk boiling due to laser activity," Pis'ma Zh. Eksp. Teor. Fiz., **52**, No. 12 (1990).
4. L. M. Lyamshev, and K. A. Naugol'nykh, "Optical generation of sound — nonlinear effects," Akust. Zh., **27**, No. 5 (1981).
5. V. F. Vitshas, V. V. Grigor'ev, V. N. Korneev, et al., "Generation of sound in the evaporation regime by the interaction of radiation with water," Akust. Zh., **31**, No. 3 (19985).
6. B. S. Maccabee, "Laser induced underwater sound," IEEE Ultrasound Symp., Colorado (1987).
7. S. V. Egerev, K. A. Naugol'nykh, A. V. Pashin, and V. N. Uchastnov, "Thermooptical emitter of sound in a two-phase medium," Akust. Zh., **30**, No. 3 (1984).
8. G. B. Crawford and D. M. Farmer, "On the spatial distribution of ocean bubbles," J. Geophys. Res. C, **92**, No. C8 (1987).
9. S. Vagle and D. M. Farmer, "The measurement of bubble size distribution by acoustical backscattering," Rept. Inst. Ocean Sci., Sydney (1991).
10. E. A. Powell, "Survey of scattering, attenuation and size spectra studies of bubble layers and plumes beneath the air−sea interface," Naval Res. Lab. Rept. 6823, Washington (1991).
11. H. Medwin and N. Breitz, "Ambient and transient bubble spectral densities in quiescent seas and under spilling breaks," J. Geophys. Res. C, **94**, No. C9 (1989).
12. B. D. Johnson and R. C. Cook, "Bubble population and spectra in coastal waters — a photographic approach," J. Geophysical Res., No. C7 (1979).
13. S. C. Ling and H. P. Pao, "Study of microbubbles in the North Sea," in: B. R. Kerman (ed.), Sea Surface Sound, Dodrecht: Klumer (1988).
14. Y. Su, S. C. Ling, and J. Cartwill, "Optical microbubble measurements in the North Sea," in: B. R. Kerman (ed.), Sea Surface Sound, Dodrecht: Klumer (1988).
15. E. A. Skelton and W. J. Fitzgerarlk, "An invariant imbedding approach to the scattering of sound from a two-phase fluid," J. Acoust. Soc. Amer., **84**, No. 2 (1988).
16. M. L. Hall, "A comprehensive model of wind-generated bubbles in the ocean and predictions of the effects of sound propagation at frequencies up to 40 kHz," J. Acoust. Soc. Amer., **86**, No. 3 (1989).
17. D. M. Farmer and S. Vagle, "Waveguide propagation of ambient sound in the ocean surface bubble layer," J. Acoust. Soc. Amer., **86**, No. 5 (1989).
18. L. M. Lyamshev, "Optoacoustic sources of sound," Usp. Fiz. Nauk, **135**, No. 4 (1981).
19. V. N. Korneev and Yu. I. Sentsov, "Modeling of the evaporation regime of the action of radiation on a fluid with a distributed surface layer," Akust. Zh., **33**, No. 4 (1987).
20. T. A. Dudina, S. V. Egerev, L. M. Lyamshev, and K. A. Naugol'nykh, "Nonlinear theory of the thermal mechanism of sound generation by laser radiation," Akust. Zh., **25**, No. 4 (1979).
21. A. I. Bozhko, F. V. Bunkin, Al. A. Kolomenskii, et al., "Laser excitation of intense sound," Tr. Fiz. Inst. Akad. Nauk — Studies in Hydrodynamics, **156** (1984).
22. M. W. Sigrist, "Laser generation of acoustic waves in liquids and gases," J. Appl. Phys., **60**, No. 7 (1986).
23. L. A. Vainshtein, "Pulse propagation," Usp. Fiz. Nauk, **118**, No. 2 (1976).
24. M. Elyses and F. Garcia-Moliner, "Propagation of wave packets," in: W. P. Mason (ed.), Physical Acoustics — Principles and Methods, Academic Press (1968), Vol. 5.
25. L. D. Landau and E. M. Lifshitz, Fluid Mechanics, 2nd rev. ed., Pergamon Press (1989).
26. V. K. Kedrinskii, "Disturbance propagation in a fluid containing gas bubbles," Prikl. Mekh. Tekh. Fiz., No. 5 (1968).
27. V. E. Nakoryakov, B. G. Pokusaev, and I. R. Shreiber, Wave Propagation in Gas- and Vapor-Fluid Media [in Russian], IT SO AN SSSR, Novosibirsk (1983).